Escaping Detrimental Interactions with Microwave-Dressed Transmon Qubits

Z. T. Wang(王子婷)[1,2], Peng Zhao(赵鹏)[3*], Z. H. Yang(杨钊华)[1,2], Ye Tian(田野)[1], H. F. Yu(于海峰)[3,4], and S. P. Zhao(赵士平)[1,2,4,5,6*]

[1]*Beijing National Laboratory for Condensed Matter Physics, Institute of Physics, Chinese Academy of Sciences, Beijing 100190, China*
[2]*School of Physical Sciences, University of Chinese Academy of Sciences, Beijing 100190, China*
[3]*Beijing Academy of Quantum Information Sciences, Beijing 100193, China*
[4]*Hefei National Laboratory, Hefei 230088, China*
[5]*CAS Center for Excellence in Topological Quantum Computation, University of Chinese Academy of Sciences, Beijing 100190, China*
[6]*Songshan Lake Materials Laboratory, Dongguan 523808, China*

(Received 5 May 2023; accepted manuscript online 27 June 2023)

Superconducting transmon qubits with fixed frequencies are widely used in many applications due to their advantages of better coherence and less control lines compared to the frequency tunable qubits. However, any uncontrolled interactions with the qubits such as the two-level systems could lead to adverse impacts, degrading the qubit coherence and inducing crosstalk. To mitigate the detrimental effect from uncontrolled interactions between qubits and defect modes in fixed-frequency transmon qubits, we propose and demonstrate an active approach using an off-resonance microwave drive to dress the qubit and to induce the ac-Stark shift on the qubit frequency. We show experimentally that the qubit frequency can be tuned well away from the defect mode so that the impact on qubit coherence is greatly reduced while maintaining the universal controls of the qubit initialization, readout, and single-qubit gate operations. Our approach provides an effective way for tuning the qubit frequency and suppressing the detrimental effect from the defect modes that happen to be located close to the qubit frequency.

DOI: 10.1088/0256-307X/40/7/070304

The precise control and manipulation of superconducting qubits are one of the key tasks in the implementation of quantum information processing.[1] Nevertheless, several uncontrolled interactions with the qubits exist due to the presence of defect modes, such as two-level systems (TLSs) in amorphous solids[2] and the chip or package modes residing in the qubit device or its package.[3–5] These uncontrolled interactions between the qubits and defect modes can cause gate errors through degrading qubit coherence[6–9] and inducing crosstalk,[3,5] thus posing serious challenges for implementing high-fidelity quantum gate operations. Such an issue will become more serious for large-scale superconducting quantum computing, since the defect modes could be increasingly prevalent in large-scale quantum devices.[3,5,6,9]

These defect modes, in general, act as hidden modes that cannot be addressed and controlled directly,[2,10] and their physical origins are often not well understood. Therefore, an active approach, such as tuning the qubit away from the defect modes, could be a practical solution to effectively turning off the qubit-defect coupling. In this way, the detrimental impact of the defect mode could be mitigated. Indeed, this approach has been demonstrated in superconducting quantum processors utilizing frequency-tunable qubits.[11] However, for the fixed-frequency qubits, which have been demonstrated as a promising qubit architecture with long coherence times and simplified controls for quantum computing,[1,12–17] there is still a pressing need for addressing the issue to prevent undermining the qubit performance when a defect mode appears close to the fixed qubit frequency.

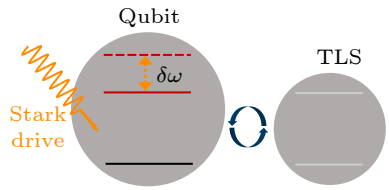

Fig. 1. Illustration of tuning the qubit frequency away from a TLS defect mode through an off-resonance drive induced ac-Stark shift $\delta\omega$.

In this work, we demonstrate experimentally an active approach that mitigates the defect-induced detrimental impacts on fixed-frequency qubits. In this approach,[18] an off-resonance microwave drive (hereafter called Stark drive) is used to dress the qubit, forming the microwave-dressed qubit,[19,20] and induce an ac-Stark shift of the qubit frequency,[9,21] as illustrated in Fig. 1. Thus, the approach provides an additional control for effectively tuning the frequency of the fixed-frequency qubit (we note that the Stark shift is also used to cancel ZZ interaction between fixed-frequency qubits, see, e.g., Refs. [22,23]). By performing the Ramsey fringe measurement under the

*Corresponding authors. Email: shangniguo@sina.com; spzhao@iphy.ac.cn
© 2023 Chinese Physical Society and IOP Publishing Ltd

Stark drive, the frequency of the dressed qubit and the ac-Stark shifts can be extracted. We further characterize the qubit coherence times and demonstrate the universal controls of the microwave-dressed qubit, including qubit initialization, readout, and single-qubit gate operations. Our results show that the qubit frequency can be effectively tuned away for more than 20 MHz with negligible effects on the qubit coherence and its universal controls. Finally, we use a nearby on-resonance qubit as an artificial (coherent) defect mode and demonstrate the effective mitigation of its detrimental impact using the present approach.

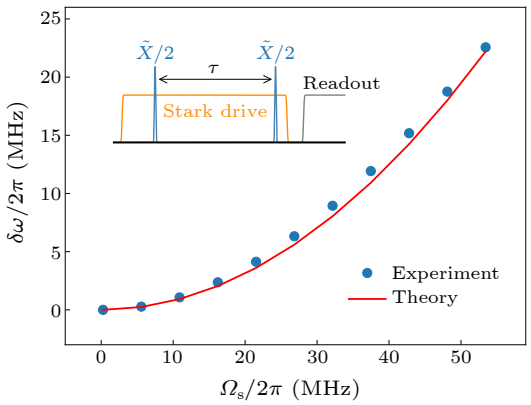

Fig. 2. The ac-Stark shift $\delta\omega$ as a function of the Stark drive amplitude Ω_s. The $\delta\omega$ is extracted from the Ramsey fringe experiment (dots) in the presence of Stark drive with the pulse sequence shown in the inset. The data are well described by the theoretical prediction (line) of Eq. (1).

In our experiment, we use a frequency-tunable transmon qubit [24] in a 21-qubit quantum chip with tunable couplers fabricated using the flip-chip technology, [25] and a standard measurement setup, [26] which are further described in the Supplemental Material. A qubit with tunable frequency is used for the convenience that, while it can be biased at a frequency to mimic the fixed-frequency qubit, it can also be biased at different frequencies to study the effect of an on-resonant artificial defect mode of a nearby qubit coupled via the tunable coupler between them. The qubit has an anharmonicity of $\alpha/2\pi = -284$ MHz and is biased at the frequency $\omega_q/2\pi = 5.330$ GHz at the sweet point. With an applied off-resonance microwave drive, i.e., the Stark drive, the qubit is dressed with shifted frequency $\tilde{\omega}_q = \omega_q + \delta\omega$, where $\delta\omega$ denotes the ac-Stark shift, which can be approximated in the low drive limit by [9,18,27]

$$\delta\omega \approx \frac{\alpha\Omega_s^2}{2\Delta(\Delta+\alpha)}, \tag{1}$$

where Ω_s is the amplitude of the Stark drive, $\Delta = \omega_q - \omega_s$ is the detuning of the bare qubit frequency ω_q from the drive frequency ω_s. In this work, we have $\omega_s = 5.230$ GHz, giving rise to $\Delta/2\pi = 100$ MHz. Figure 2 shows the measured ac-Stark shift $\delta\omega$ as a function of Ω_s (symbols), which displays a clear quadratic dependence on the drive amplitude and agrees well with the theoretical prediction (line) of Eq. (1). In Fig. 2, Ω_s represents the Rabi frequency for the applied microwave amplitude and $\delta\omega$ is extracted from the Ramsey fringe measurement under the always-on Stark drive with the experimental pulse sequence illustrated in the inset ('always-on' means the absence of the drive only during readout). The results clearly show that by using the Stark drive with a moderate drive amplitude, the qubit frequency can be effectively tuned away from its original value for more than 20 MHz. [28]

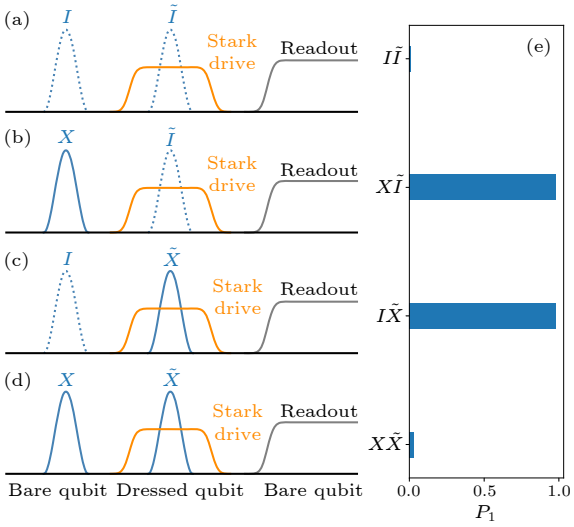

Fig. 3. The qubit initialization, gate operation, and readout for the demonstration of the equivalence of qubit controls with and without the Stark drive. (a)–(d) The pulse sequences for the experiment with results shown in (e). The drive has the amplitude with $\delta\omega/2\pi = 20$ MHz. Here I and X refer to the identity and bit-flip gates, respectively, and $\tilde{I}$ and $\tilde{X}$ represent the corresponding gates under the Stark drive. Nothing is performed with the I and $\tilde{I}$ gates which are illustrated by dashed curves. P_1 denotes the population of the qubit first excited state.

We test controls over the qubit including initialization, gate operation, and readout, and demonstrate the equivalence of the controls with and without the Stark drive. To do so, the Stark drive amplitude is slowly ramped up and down so that the bare and dressed qubit states can be adiabatically mapped to each other. [18,29,30] Figures 3(a)–3(d) illustrate the pulse sequences to implement the universal controls with four different combinations of identity (I and $\tilde{I}$) and bit-flip (X and $\tilde{X}$) gates without and with the drive. Experimentally, the qubit is first prepared in its ground or excited states. The Stark drive amplitude is then ramped up to a certain value and a specific gate is performed. After the ramp-down process, we finally measure the qubit state. Generally, a long ramping time makes the state map between the bare qubit and the dressed qubit more perfect, thus improving the fidelity of the initialization and readout of the dressed qubit. [18,30] In this work, the ramp-up and ramp-down processes follow an error function with a ramp time of 50 ns. Both the X and $\tilde{X}$ gates for the bare and dressed qubits are optimized using the derivative removal by adiabatic gate (DRAG) scheme with cosine-shaped pulses [18,31] leading to fidelities around 99.85% (see below). Here we use pulses with relatively long length of 40 ns, which have a longer duration interacting with the driving signal and therefore partly reduce the fidelity. Figure 3(e) shows the experimental results. We find that the fidelities of the qubit state initialization and readout range

from 97.1% up to 99.0%, and the gate performance can be optimized with high quality in both cases with and without the Stark drive.

The relaxation time T_1 and Ramsey dephasing time T_2^* are measured to examine the coherence properties of the microwave-dressed qubit. The Stark drive is always-on in the measurement, similar to the case shown in the inset of Fig. 2. In order to avoid misinterpretation due to the possible fluctuations of the qubit [6–9] or the measurement electronics, the T_1 and T_2^* measurements are performed alternately. Namely, one is measured for five different values of $\delta\omega$ followed by the measurements of the other. For the T_1 measurement, the dressed qubit is first excited by applying an $\tilde{X}$ gate, and then the qubit state is measured with varying time delays. The T_2^* time is extracted from the Ramsey experiment, where two $\tilde{X}/2$ gates separated by varying the time delay are applied to the dressed qubit, and finally the qubit state is measured, as can be seen in the inset of Fig. 2. In Figs. 4(a) and 4(c), we present the T_1 and T_2^* times with varying ac-Stark shift $\delta\omega$, respectively, from the alternate measurements over ~ 10 h. Typical results of the relaxation and Ramsey fringe with $\delta\omega/2\pi = 20$ MHz are presented in Figs. 4(b) and 4(d). From the measured T_1 data, we find that with the Stark drive, T_1 shows a moderate improvement. This may result from the possible existence of the fluctuating TLS modes located close to the bare qubit frequency, which are nearly on-resonantly coupled to the qubit and thus reduce the qubit relaxation time. By effectively tuning the qubit away from the TLS modes with the Stark drive, the qubit relaxation time is improved. [32] For the Ramsey dephasing time T_2^*, there appears only a slight degradation, which may be attributed to the amplitude noise of the Stark drive. [33,34] In any case, we can conclude that the coherence times are not much changed by the applied Stark drive.

We now turn to characterize the performance of the gate operation for the microwave-dressed qubit. The fidelity of the single-qubit gate optimized with the DRAG scheme described above is characterized using the standard randomized benchmarking (RB) technique. [35,36] We only use 20-ns-long $\pi/2$-pulses ($\pm\tilde{X}/2$ and $\pm\tilde{Y}/2$) in single-qubit RB experiments, giving rise to 2.2083 physical gates per single-qubit Clifford gate on average. Figure 4(e) shows the averaged single-qubit gate errors with varying Stark shifts, while in Fig. 4(f), the typical RB curve with the Stark shift of $\delta\omega/2\pi = 20$ MHz is presented. We find that with the Stark drive, the gate performance generally does not show any significant degradation (the added error is below 2.5×10^{-4}). These results demonstrate that using the Stark drive, the qubit frequency can be effectively tuned up to 20 MHz while retaining minimal impacts on the qubit coherence and the performance of gate operation over the dressed qubit.

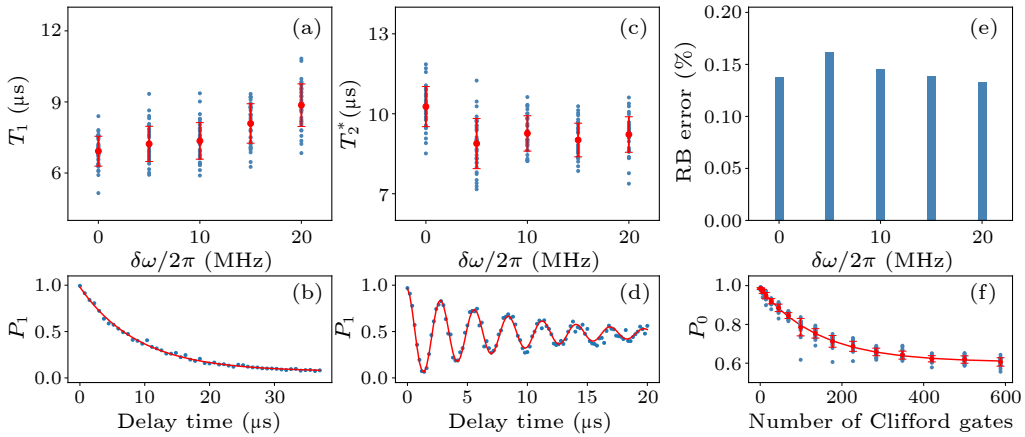

Fig. 4. Characterization of the qubit coherence and single-qubit gate performance with varying ac-Stark shifts. (a) The relaxation time T_1, (c) the dephasing time T_2^*, measured alternately over 10 h. The error bars are the standard deviations of the mean values (red dots) averaged over 38 measurements. (e) The average single-qubit gate errors obtained from the randomized benchmarking (RB) technique. In (b), (d), and (f), the relaxation curve, the Ramsey fringe curve, and the RB curve measured with $\delta\omega/2\pi = 20$ MHz are given, respectively.

To further examine the feasibility of using the Stark drive to mitigate the defect-induced detrimental impact on qubits, we introduce an artificial coherent defect mode, i.e., a nearby qubit on the same chip, which is on-resonantly coupled to the qubit studied above (see the Supplemental Material). The qubit-'defect' interaction can be adjusted by controlling the frequency of the coupler between them. [37] With the presence of the artificial defect, we again characterize the qubit coherence time and the single-qubit gate performance. To make an on-resonant coupling between qubit and defect, we bias the qubit away from its sweet point, which does not change the qubit relaxation time T_1 but reduce the dephasing time T_2^* from around 9 μs to about 2 μs. Figure 5 shows the experimental results with the qubit-defect coupling strength of $g/2\pi = 0.5$ MHz. In Fig. 5(a), without the Stark drive, a clear population swap process between qubit and defect can be found in the qubit relaxation curve. When the Stark drive with $\delta\omega/2\pi = 20$ MHz is applied, the population swap disappears. From the Ramsey fringes shown in

Fig. 5(b), we find that the presence of the defect produces a clear beating feature of the bare qubit, and when the Stark drive is on, the typical damped sinusoid appears. We note that the fitted results of $T_1 = 7.878\,\mu s$ and $T_2^* = 2.0\,\mu s$ are obtained from the data in Figs. 5(a) and 5(b) with Stark drives. These results indicate that the Stark drive effectively removes the detrimental impact from the defect with coherence times T_1 and T_2^* basically unaffected.

Finally, we can see the benefit of using the Stark drive from the RB results in the presence of the artificial defect, as shown in Figs. 5(c) and 5(d). With the applied Stark drive in Fig. 5(d), the performance of the implemented single-qubit gate indeed shows an improvement over the result without the Stark drive in Fig. 5(c) (99.76% vs 99.72%). Moreover, from the RB curves, we find that without the Stark drive, the RB data show more prominent scatter, suggesting the gate-dependent error, i.e., the coherent error, contributing significantly to the gate error.[38] On the contrary, with the Stark drive, the scatter is seen to be much suppressed.

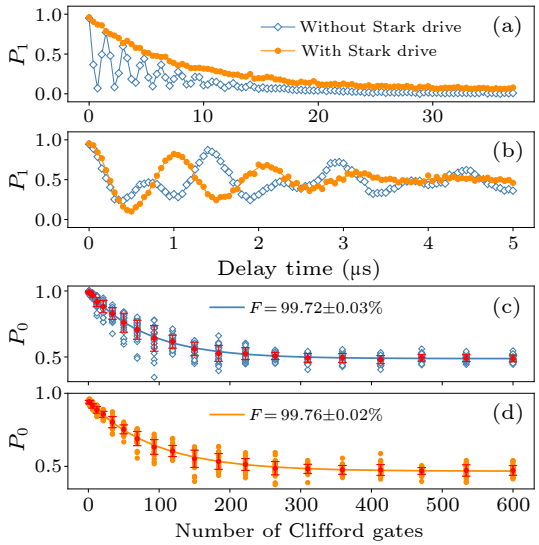

Fig. 5. Mitigating the detrimental impact of an artificial coherent defect coupled resonantly to the qubit with coupling strength of ~ 0.5 MHz. (a) Energy relaxation. (b) Ramsey fringe. $T_1 = 7.878\,\mu s$ and $T_2^* = 2.0\,\mu s$ are obtained from the data with Stark drives. [(c), (d)] The RB results without and with the Stark drive, respectively.

In summary, we have experimentally explored the possibility of mitigating the defect-induced detrimental impact on fixed-frequency qubits by using an ac-Stark drive to dress the qubit. It is realized that by applying an off-resonance Stark drive, the qubit frequency can be effectively tuned away for more than 20 MHz while keeping minimal influences on the qubit coherence as well as the qubit controls including initialization, readout, and gate operations.[39] With a nearby qubit on the the same chip serving as an artificial (coherent) defect, we also realize that by tuning away the qubit frequency, the effect from the defect mode could be largely suppressed. Our work demonstrates that the active approach based on the qubit dressing by an ac-Stark drive could be used to escape the detrimental interactions from the defect modes located close to the qubit fixed frequency, as long as they are static or do not change with time quickly. While in the present work, our demonstration of the universal control over the dressed qubit is restricted to the single-qubit system, similar consideration would apply for the two-qubit gate operations with dressed qubits in multiqubit system, as theoretically explored recently.[18,34]

Acknowledgments. We acknowledge helpful discussions with Weizhou Cai. This work was partly supported by the National Natural Science Foundation of China (Grant Nos. 12204050, 11890704, and 12004042), the Beijing Natural Science Foundation (Grant No. Z190012), and the Key-Area Research and Development Program of Guang Dong Province (Grant No. 2018B030326001).

References

[1] Krantz P, Kjaergaard M, Yan F, Orlando T P, Gustavsson S, and Oliver W D 2019 *Appl. Phys. Rev.* **6** 021318
[2] Müller C, Cole J H, and Lisenfeld J 2019 *Rep. Prog. Phys.* **82** 124501
[3] Wenner J, Neeley M, Bialczak R C, Lenander M, Lucero E, ÓConnell A D, Sank D, Wang H, Weides M, Cleland A N, and Martinis J M 2011 *Supercond. Sci. Technol.* **24** 065001
[4] Rosenberg D, Weber S, Conway D, Yost D, Mallek J, Calusine G, Das R, Kim D, Schwartz M, Woods W, Yoder J L, and Oliver W D 2019 arXiv:1906.11146 [quant-ph]
[5] Huang S, Lienhard B, Calusine G, Vepsäläinen A, Braumüller J, Kim D K, Melville A J, Niedzielski B M, Yoder J L, Kannan B, Orlando T P, Gustavsson S, and Oliver W D 2021 *PRX Quantum* **2** 020306
[6] Klimov P V, Kelly J, Chen Z *et al.* 2018 *Phys. Rev. Lett.* **121** 090502
[7] Burnett J J, Bengtsson A, Scigliuzzo M, Niepce D, Kudra M, Delsing P, and Bylander J 2019 *npj Quantum Inf.* **5** 54
[8] Schlör S, Lisenfeld J, Müller C, Bilmes A, Schneider A, Pappas D P, Ustinov A V, and Weides M 2019 *Phys. Rev. Lett.* **123** 190502
[9] Carroll M, Rosenblatt S, Jurcevic P, Lauer I, and Kandala A 2022 *npj Quantum Inf.* **8** 132
[10] Sheldon S, Sandberg M, Paik H, Abdo B, Chow J M, Steffen M, and Gambetta J M 2017 *Appl. Phys. Lett.* **111** 222601
[11] Kelly J, Barends R, Fowler A G, Megrant A, Jeffrey E, White T C, Sank D, Mutus J Y, Campbell B, Chen Y U, Chen Z, Chiaro B, Dunsworth A, Hoi I C, Neill C, O'Malley P J J, Quintana C, Roushan P, Vainsencher A, Wenner J, Cleland A N, Martinis J M 2015 *Nature* **519** 66
[12] Xu Y, Chu J, Yuan J, Qiu J, Zhou Y, Zhang L, Tan X, Yu Y, Liu S, Li J, Yan F, Yu D P 2020 *Phys. Rev. Lett.* **125** 240503
[13] Stehlik J, Zajac D M, Underwood D L, Phung T, Blair J, Carnevale S, Klaus D, Keefe G A 2021 *Phys. Rev. Lett.* **127** 080505
[14] Kandala A, Wei K X, Srinivasan S, Magesan E, Carnevale S, Keefe G A, Klaus D, Dial O, and McKay D C 2021 *Phys. Rev. Lett.* **127** 130501
[15] Place A P M, Rodgers L V H, Mundada P *et al.* 2021 *Nat. Commun.* **12** 1779
[16] Wang C, Li X, Xu H *et al.* 2022 *npj Quantum Inf.* **8** 3
[17] Gordon R T, Murray C E, Kurter C *et al.* 2022 *Appl. Phys. Lett.* **120** 074002
[18] Zhao P, Ma T, Jin Y, and Yu H F 2022 *Phys. Rev. A* **105** 062605
[19] Cohen-Tannoudji C, Dupont-Roc J, and Grynberg G 1998 *Atom-Photon Interactions* (New York: Wiley)
[20] Liu Y X, Sun C P, and Nori F 2006 *Phys. Rev. A* **74** 052321
[21] Oelsner G, Hübner U, and Il'ichev E 2020 *Phys. Rev. B* **101** 054511
[22] Mitchell B K, Naik R K, Morvan A *et al.* 2021 *Phys. Rev. Lett.* **127** 200502

[23] Ni Z, Li S, Zhang L *et al.* 2022 *Phys. Rev. Lett.* **129** 040502
[24] Koch J, Yu T M, Gambetta J, Houck A A, Schuster D I, Majer J, Blais A, Devoret M H, Girvin S M, and Schoelkopf R J 2007 *Phys. Rev. A* **76** 042319
[25] Li X G, Zhang Y, Yang C, Li Z Y *et al.* 2021 *Appl. Phys. Lett.* **119** 184003
[26] Li X G, Xu H K, Wang J H, Tang L Z *et al.* 2023 arXiv:2301.12138 [quant-ph]
[27] Schneider A, Braumüller J, Guo L, Stehle P, Rotzinger H, Marthaler M, Ustinov A V, and Weides M 2018 *Phys. Rev. A* **97** 062334
[28] The output power of the microwave source giving the qubit frequency shift of 20 MHz is close to the maximum value of the instrument.
[29] Seedhouse A E, Hansen I, Laucht A, Yang C H, Dzurak A S, and Saraiva A 2021 *Phys. Rev. B* **104** 235411
[30] Huang Z, Mundada P S, Gyenis A, Schuster D I, Houck A A, and Koch J 2021 *Phys. Rev. Appl.* **15** 034065
[31] Motzoi F, Gambetta J M, Rebentrost P, and Wilhelm F K 2009 *Phys. Rev. Lett.* **103** 110501
[32] Lisenfeld J, Bilmes A, and Ustinov A 2022 *Preprint* (Version 1) available at https://doi.org/10.21203/rs.3.rs-1815706/v1
[33] Wei K X, Magesan E, Lauer I, Srinivasan S, Bogorin D F, Carnevale S, Keefe G A, Kim Y, Klaus D, Landers W, Sundaresan N, Wang C, Zhang E J, Steffen M, Dial O E, McKay D C, and Kandala A 2021 arXiv:2106.00675 [quant-ph]
[34] Zhao P, Wang R, Hu M J, Ma T, Xu P, Jin Y, and Yu H F 2023 *Phys. Rev. Appl.* **19** 054050
[35] Magesan E, Gambetta J, and Emerson J M 2011 *Phys. Rev. Lett.* **106** 180504
[36] Magesan E, Gambetta J M, Johnson B R, Ryan C A, Chow J M, Merkel S T, Silva M P D, Keefe G A, Rothwell M B, Ohki T A, Ketchen M B, and Steffen M 2012 *Phys. Rev. Lett.* **109** 080505
[37] Yan F, Krantz P, Sung Y, Kjaergaard M, Campbell D L, Orlando T P, Gustavsson S, and Oliver W D 2018 *Phys. Rev. Appl.* **10** 054062
[38] Knill E, Leibfried D, Reichle R, Britton J, Blakestad R B, Jost J D, Langer C, Ozeri R, Seidelin S, and Wineland D J 2008 *Phys. Rev. A* **77** 012307
[39] We mention that the Stark drive is always off during readout in the present work. However, it can also be applied during readout as demonstrated theoretically. [34]